DOI:10.1021/jf904508g

JOURNAL OF AGRICULTURAL AND FOOD CHEMISTRY
ARTICLE

Production, Refining, Structural Characterization and Fermentability of Rice Husk Xylooligosaccharides

Patricia Gullón,[†,‡] María Jesús González-Muñoz,[†,‡] Martine Paula van Gool,[§] Henk Arie Schols,[§] Ján Hirsch,[∥] Anna Ebringerová,[∥] and Juan Carlos Parajó*[,†,‡]

[†]Department of Chemical Engineering, Faculty of Science, University of Vigo (Campus Ourense), As Lagoas, 32004 Ourense, Spain, [‡]CITI-Tecnopole, San Ciprián de Viñas, 32901 Ourense, Spain, [§]Laboratory of Food Chemistry, Wageningen University, Bomenweg 2, 6703 HD, Wageningen, The Netherlands, and [∥]Institute of Chemistry, Center for Glycomics, Slovak Academy of Sciences, Dúbravská cesta 9, SK-845 38 Bratislava, Slovakia

Oligosaccharides produced by hydrothermal processing of rice husks (xylooligosaccharides and glucooligosaccharides) were refined by membrane processing (operating in diafiltration and concentration modes), subjected to xylanase treatment to reduce the average molar mass, and subjected to further purification by ultrafiltration (operating in concentration mode) and ion exchange. The purified products were assayed for composition, molar mass distribution and structural characterization by HPLC, HPAEC-PAD, HPSEC, MALDI-TOF-MS and NMR (^{1}H and ^{13}C). The fermentability of the purified product by fecal inocula was assessed on the basis of the time courses of pH and oligosaccharide concentrations. Succinate, lactate, formiate, acetate, propionate and butyrate were the major products resulting from fermentation experiments.

KEYWORDS: Fermentation; refining; rice husks; structure; xylooligosaccharides

INTRODUCTION

There are a variety of lignocellulosic substrates (such as hardwoods, hulls, brans, corn cobs and corn stover, industrial byproducts like brewery spent grains and shells) whose hemicellulosic fraction is mainly made up of xylan, a polymer made up of a β-(1−4)-D-xylopyranose backbone. In native feedstocks, xylan can be substituted (for example, with arabinosyl, acetyl, uronic of phenolic groups). Xylooligosaccharides (XOS) can be produced from this kind of lignocellulosic raw material by treatment with hot, compressed water (autohydrolysis) (*1*−*3*). During autohydrolysis treatment, xylan is broken down into a variety of soluble products (including monosaccharides, XOS and compounds of higher molar mass). Both the molar mass distribution and the substitution pattern of XOS depend on both the raw material employed and the severity of the operational conditions (*2*, *4*).

From a nutritional point of view, XOS behave as nondigestible oligosaccharides (NDO), which are not degraded in the stomach and reach the large bowel intact, where they are degraded by the intestinal microbiota (*5*). XOS are classified as "emerging prebiotics", presenting a promising prebiotic potential although they still lack strong scientific evidence (*6*).

A prebiotic is a nonviable food component that confers a health benefit on the host associated with modulation of the intestinal microbiota (*7*). Many studies have confirmed that prebiotics are a valid approach to the dietary modulation of the colonic microbiota: in addition to the desirable increase in bifidobacteria and lactobacilli, short-chain fatty acids (SCFA) are end products of oligosaccharide fermentation. The profile of such SCFA varies between oligosaccharides and contains greater or lesser quantities of propionate and butyrate. Both compounds have been implicated in a number of important physiological events (including bowel function, calcium absorption, lipid metabolism, reduction of the risk of colon cancer) (*8*).

The interest in producing XOS lies mainly on their utilization as food ingredients. Food applications require high-purity XOS, which are already commercial products with market prices higher than other NDO (*9*). To use autohydrolysis-derived XOS as food ingredients, the contaminating undesired compounds from the reaction medium must be removed. These undesired products include non-saccharide fractions derived from extractives, acid-soluble lignin, and inorganic components.

For this purpose, membrane technologies have been employed (*10*). Ultrafiltration leads to the separation of oligosaccharides (OS) from higher molar mass products or to fractionate OS of different DP (*11*). On the other hand, nanofiltration can be useful for concentrating liquors and/or for removing undesired low molar mass compounds, such as monosaccharides or phenolics, enabling the purification of OS mixtures (*12*).

This work deals with (a) the manufacture of high-purity XOS by physicochemical processing of liquors obtained by rice husks autohydrolysis; (b) the structural characterization of the purified product; and (c) the fermentability of the purified product by fecal inocula.

*Author to whom correspondence should be addressed. Phone: +34988387033 Fax: +34988387001. E-mail: jcparajo@uvigo.es.

 Published on Web 02/17/2010

MATERIALS AND METHODS

Raw Material and Autohydrolysis Conditions. Rice husks from a local factory (*Procesadora Gallega de Alimentos*, Lalín, Pontevedra, Spain) were air-dried, homogenized in a single lot to avoid differences in composition among aliquots, and stored. Aliquots from the above homogenized lot were mixed with water at the desired proportions (8 kg/kg oven dry solid) and reacted in a Parr reactor fitted with double six-blade turbine impellers. The vessel was heated with external fabric mantles, and cooled with an internal stainless steel loop. Temperature was monitored using an inner thermocouple, and controlled by a PID module. Isothermal reaction was carried out using the fastest heating profile of the reactor to achieve 185 °C during 20 min, conditions under which the XOS concentration was maximal (*13*).

Refining of Autohydrolysis Liquors. *Membrane Processing*. The experimental setup consisted of an 8 L tank with a coil for temperature control, a diaphragm pump (Hydra-cell, Wanner Engineering Inc.) used to feed liquors to the membrane module, a membrane housing, two pressure gauges at the membrane inlet and outlet to measure the transmembrane pressure (TMP), a needle valve located after the membrane to achieve the desired TMP, and a flowmeter to measure the recirculation flow. Tubular ceramic membranes (Tami Industries) with 0.022 m^2 of filtration area and cutoffs of 1 kDa and 15 kDa were used in experiments. The maximum allowed TMP was 10 bar. Assays were carried out in diafiltration and concentration modes.

Preliminary experiments were carried out in full recycle mode operating at TMP in the range 2−10 bar. Further experiments were carried out in diafiltration mode at TMP of 8 bar, and in concentration mode at TMP of 10 bar using a ceramic membrane with cutoff of 1 kDa. Retentates from the experiments performed in concentration mode were subjected to further enzymatic processing, and to concentration with a membrane with cutoff of 15 kDa (TMP, 4 bar). The corresponding permeate was purified by anionic exchange, as described below.

Enzymatic Processing. Retentates from the membrane concentration assays were treated with commercial endoxylanases (Pulpzyme HC) kindly provided by Novozymes-Spain. The endoxylanase activity of the commercial concentrate was measured by the Megazyme assay (Megazyme International Ireland Ltd., Wicklow, Ireland), based on the depolymerization of Remazol Brilliant Blue (RBB), and converted into xylanase units (XU) using the method provided by the manufacturer. The activity of Pulpzyme HC was 1714 XU/mL. Commercial xylanases were added to the concentrate at the desired enzyme loading (685 XU/kg liquor), and the solution was set at pH 7 and shaked at 120 rpm and 55 °C for 48 h.

Ion Exchange Processing. Processed liquors were treated with Amberlite IRA 96 (a weak anion-exchange resin) for removing undesired, noncarbohydrate compounds. Liquors and resin were contacted overnight with gentle agitation at room temperature using a mass ratio resin:liquor of 1/15. The resulting liquors were freeze-dried before storage, and diluted at the desired proportions to yield the culture media.

Fermentation of Purified XOS. Fermentation of XOS from rice husk autohydrolysis was performed using an inoculum made from fresh feces collected from a healthy human volunteer, who usually ingested a normal diet, presented no digestive diseases and did not receive antibiotics for at least 3 months. Feces were collected into sterile vials, which were sealed and maintained at 37 °C until inoculum was prepared for the fermentation assay (not exceeding 2 h after collection). The fecal inoculum (FI) was diluted in reduced physiological salt solution (RPS, cysteine-HCl 0.5 g/L and NaCl 8.5 g/L) in a ratio of 10% w/v. Before use, and during preparation of the inoculum, anaerobiosis and pH (6.8) were maintained by continuous bubbling of CO_2 and N_2. The slurry was mixed and homogenized for 2 min under CO_2 and N_2 stream. Blended, diluted feces were filtered through four layers of surgical gauze to remove nondigested materials and transferred to serum bottles (*14*, *15*).

The nutrient base medium used in fermentation experiments was prepared as described previously (*12*): the medium was deoxygenated with CO_2 and N_2 using a gassing manifold system, and pH was adjusted to 6.8. Nine milliliter aliquots were distributed into airtight anaerobic culture tubes (Bellco Biotechnology Inc., Vineland, NJ), which were capped with butyl rubber stoppers and sealed with aluminum caps before autoclave sterilization. Anaerobic stock solutions of Yeast Nitrogen Base (YNB) and XOS were prepared in airtight serum bottles and distributed into the culture tubes, to final concentrations about of 5 g/L and 10 g/L of freeze-dried powder, respectively. The tubes with the fermentation medium were inoculated with 0.2 mL of intestinal dilution in triplicate and incubated at 37 °C for 48 h without shaking. Bacterial growth was monitored at 600 nm using a spectrophotometer (Thermo Spectronic Genesys 20, Garforth, U.K.). At each sampling time, cells were harvested by centrifugation and supernatants were filtered for HPLC analysis. The pH of tube contents was measured with a standard pHmeter.

Analytical Methods. *Analysis of Liquors*. Samples of liquors were filtered through 0.45 μm cellulose acetate membranes and assayed by HPLC for glucose, xylose, arabinose and acetic acid, using a 1100 series Hewlett-Packard chromatograph fitted with a refractive index detector (temperature, 50 °C). Other analysis conditions were as follows: Aminex HPX-87H column (Bio-Rad, Life Science Group, Hercules, CA); mobile phase, 0.003 M H_2SO_4; flow, 0.6 mL/min. A second sample of liquors was subjected to quantitative posthydrolysis (with 4% sulfuric acid at 121 °C for 20 min) before duplicate HPLC analysis. The increase in the concentrations of xylose and glucose caused by posthydrolysis provided a measure of the oligomers (xylooligomers and glucooligomers) present in the media. In the same way, the increase in acetic acid concentration measured the amount of acetyl groups present in the reaction products, and the increase in arabinose concentration measured the amount of arabinosyl moieties (Ara) linked to oligosaccharides. Uronic acids were determined by the method of Blumenkrantz and Asboe-Hansen (*16*) using galacturonic acid as a standard for quantification. The galacturonic acid equivalent of uronic acid substituents is denoted UA. All the analyses were made in triplicate.

Determination of Carbohydrates and Fermentation Products in Cell-Free Supernatants. Supernatants from the anaerobic culture tubes inoculated with FI were filtered through 0.22 μm cellulose acetate membranes. One aliquot was analyzed by HPLC for monosaccharides, total oligosaccharides, SCFA (acetic, formic and butyric acid, mainly) and lactate, using the method described above.

Characterization of Purified XOS (RH-XOS). *High-Performance Size Exclusion Chromatography* (*HPSEC*). The oligosaccharide molar mass distribution of RH-XOS was determined by HPSEC using an Agilent instrument fitted with a refractive index detector using two TSK-Gel columns (7.8 mm i.d. × 30 cm per column) in series ($G2500PW_{XL}$, $G3000PW_{XL}$; Tosoh Bioscience) in combination with a PWX-guard column. Elution took place at 30 °C with 0.05 M KNO_3 containing 83 mg sodium azide/L at 0.6 mL/min. Dextrans (1000−80,000 Da) from Fluka, malto-OS (DP 2 to DP 7) from Supelco and XOS (DP 2 to DP 6 from Megazymes) were used as calibration standards.

Qualitative Sugar Analysis by Paper Chromatography (*PC*). RH-XOS was hydrolyzed with 1 M TFA under reflux for 1 h. The hydrolysate was treated with cation- and anion-exchange resins (*17*) to separate the neutral and acidic sugars, which were identified by PC in solvent systems S_1, ethyl acetate/pyridine/water = 8:2:1 (v/v), for neutral sugars and S_2, ethyl acetate/acetic acid/formic acid/water = 18:3:1:4 (v/v), for acidic sugars, using authentic sugar standards.

High-Performance Anion Exchange Chromatography (*HPAEC*). RH-XOS was also analyzed by HPAEC using an ICS3000 chromatographic system (Dionex, Sunnyvale, CA), equipped with a CarboPac PA-1 column (2 mm i.d. × 250 mm) in combination with a CarboPac PA guard column (2 mm i.d. × 25 mm) and a ISC3000 PAD-detector. A flow rate of 0.3 mL/min was used with the following gradient of 0.1 M NaOH and 1 M NaOAc in 0.1 M NaOH: 0−45 min, 0−500 mM NaOAc in 0.1 M NaOH; 45−48 min washing step with 1 M NaOAc in 0.1 M NaOH; 48−60 min, equilibration with 0.1 M NaOH. The injection volume was 20 μL.

Matrix Assisted Laser Desorption/Ionization Time of Flight Mass Spectrometry (*MALDI-TOF-MS*). For the MALDI-TOF-MS analysis an Ultraflex workstation (Bruker Daltonics, Bremen, Germany) equipped with a 337 nm nitrogen laser was used. The mass spectrometer was operated in the positive mode and calibrated with a mixture of maltodextrins (AVEBE, Veendam, The Netherlands; mass range 500−3500 Da as sodium adducts). After a delayed extraction time of 120 ns, the ions were accelerated with a 25 kV voltage and subsequently detected using the reflector mode. Data were collected from averaging 200 laser shots, with the lowest energy necessary to obtain sufficient spectra intensity. For sample preparation 1 μL of desalted sample solution (1 mg/mL) was mixed with 1 μL of matrix, directly applied on the MS target plate and dried

Table 1. Composition of Streams A, C, E, H and K in **Figure 1**[a]

component	stream A	stream C	stream E	stream H	streams K/O
glucose	0.007	0.004	0.002	0.011	0.011
xylose	0.029	0.013	0.004	0.008	0.006
arabinose	0.035	0.016	0.004	0.007	0.008
glucooligosaccharides (as glucose)	0.089	0.109	0.133	0.132	0.146
xylooligosaccharides (as xylose)	0.426	0.470	0.544	0.609	0.682
arabinose substituents (as arabinose)	0.023	0.026	0.034	0.033	0.029
acetyl groups (as acetic acid equivalent)	0.029	0.035	0.042	0.043	0.039
uronic acid substituents (as galacturonic acid equivalent)	0.042	0.048	0.053	0.049	0.048
ONVC[b]	0.321	0.279	0.184	0.108	0.032
NVC[c] (kg of NVC/kg of liquor)	0.0230	0.0175	0.0680	0.0451	0.040
mass ratio (kg of stream/kg of stream A)	1	1	0.20	0.15	0.13

[a] Expressed as kg of component/kg of nonvolatile compounds NVC, except where the opposite is indicated. [b] ONVC, other nonvolatile compounds. [c] NVC, nonvolatile compounds.

under a stream of warm air. The matrix solution was prepared by dissolving 10 mg of 2,5-dihydroxybenzoic acid (Bruker Daltonics, Bremen, Germany) in a mixture of 700 μL of water and 300 μL of acetonitrile.

FT-IR and NMR Spectroscopy. FT-IR spectra (in KBr pellets) were collected on a Nicolet 6700 spectrometer equipped with a DTGS detector (high-pass filter, 20,000; low-pass filter, 11,000). Data were recorded at 15798.3 cm^{-1} resolution using 8480 scans. All NMR spectra were acquired on a VNMRS Varian spectrometer equipped with a 1H-19F/15N-31P 5 mm PFG AutoX DB NB Probe and operating at 399.89 MHz for ^1H and 100.56 MHz for ^{13}C. Measurements were performed in D_2O at 60 °C using 3-(trimethylsilyl)propanesulfonic acid sodium salt as internal standard (δ 0.00) for calibration. For both ^1H and ^{13}C NMR spectra, chemical shifts are referenced to H-1 and C-1 of 4-linked α-Glc*p* residue in maltodextrin (δ_H and δ_C: 3.55 and 100.9, respectively). The multiplicity edited $^1H-^{13}C$ HSQC spectrum was recorded in the phase-sensitive pure absorption mode with optimization on one bond coupling constant $^1J_{C,H}$ = 140 Hz using standard pulse sequences and 2 × 128 increments. Data processing was performed using the MestReNova 5.3 program.

RESULTS AND DISCUSSION

Autohydrolysis and Refining of XOS. Autohydrolysis of rice husks under suitable operational conditions leads to the depolymerization of hemicelluloses, resulting in the formation of oligosaccharides (see **Table 1**, stream A). The substituted XOS obtained in autohydrolysis treatments keep a part of the substituents present in the original xylan, similarly as observed during hydrothermal treatment of other xylan-rich plant materials (*4*). During treatments, other side processes occur, including extractive removal from solid phase, solubilization of acid-soluble lignin, dissolution of inorganic components, and saccharide conversion into dehydration products. Therefore, crude liquors have to be refined to obtain food-grade XOS (*18*).

As illustrated in **Figure 1**, the purification scheme of the raw autohydrolysis liquors included sequential steps of membrane processing (operating in diafiltration and concentration modes), endoxylanase hydrolysis (to keep the DP distribution within the desired limits), ultrafiltration, ion exchange with an anionic resin, and freeze-drying. **Table 1** lists compositional data of the resulting streams (denoted A, C, E, G and K in **Figure 1**). The same table includes the mass ratio of streams, in order to enable the calculation of recovery yields. Liquors were made up of volatile components (water and volatile reaction products) and nonvolatile compounds (NVC). The composition of streams is expressed in terms of mass fraction of the considered component referred to NVC (kg of component/kg of NVC). Since the objective of this work was to refine the process streams to increase their content of XOS (which are of nonvolatile character), the fate of volatile compounds through the process is not relevant. The NVC present in streams include monosaccharides (xylose, arabinose and glucose, which are undesired compounds for the purpose of this work), oligosaccharides (XOS and glucooligosaccharides, GOS) and arabinosyl moieties linked to oligosaccharides (Ara), which are expressed as monosaccharide equivalents; other oligosaccharide substituents (acetyl groups expressed as acetic acid, and uronic acid units, denoted UA, expressed as galacturonic acid equivalent, respectively), and other non-saccharide, nonvolatile compounds (for example, inorganic componentes, extractives and lignin-derived products, here denoted ONVC, which have to be removed). The purification process based on membrane separation assayed in this work was intended to selectively remove ONVC and monosaccharides, leading to a recovery yield of XOS and XOS substituents in the final product (here denoted RH-XOS) as high as possible.

Membrane Processing of Raw Autohydrolysis Liquors. *Continuous Diafiltration*. Preliminary nanofiltration of liquors was carried out operating in full recycle mode (data not shown) using a 1 kDa molecular weight cutoff (MWCO) ceramic membrane, in order to assess the effects of TMP along the whole experimental range (2−10 bar). On basis of the experimental information, the TMP selected for operation in diafiltration mode was 8 bar. Diafiltration proceeded up to achieve one diavolume. **Table 1** lists compositional data of the retentate (stream C in **Figure 1**). Material balances showed that the percentages of recovery in diafiltered autohydrolysis liquor with respect to stream A were 35−45.5% for monosaccharides, in comparison with 93.2% for GOS, 84% for XOS, 85% for Ara, 92.4% for acetyl groups linked to oligosaccharides, and 86.6% for UA. Just 66.2% of the initial ONVC amount was kept in diafiltered autohydrolysis liquors, leading to a decreased ONVC mass fraction in stream C (0.279) in comparison with stream A (0.321). These data confirm purification effects caused by diafiltration, derived from the preferential removal of both monosaccharides and ONVC in permeate.

Nanofiltration in Concentration Mode. According to **Figure 1**, stream C from diafiltration was subjected to nanofiltration in concentration mode using the same membrane. **Table 1** lists data on the composition of the retentate (stream E in **Figure 1**) obtained at a VRC of 5 (5-fold volume reduction). Material balances showed that the percentages of recovery after diafiltration and concentration with respect to stream A were 7.5−18.2% for monosaccharides, in comparison with 87.9% for GOS, 75.5% for XOS, 86.8% for Ara, 87.3% for acetyl groups, and 73.6% for UA. Just 37.5% of the initial ONVC fraction was kept in retentate (diafiltered autohydrolysis liquor), confirming the ability of this processing step for additional purification, confirmed by a reduction in the mass fraction of ONCV from 0.32 up to 0.18.

Enzymatic Hydrolysis, Ultrafiltration in Mode Concentration and Diafiltration. Along autohydrolysis treatments, the xylan chains are broken down randomly, leading to hydrolysis

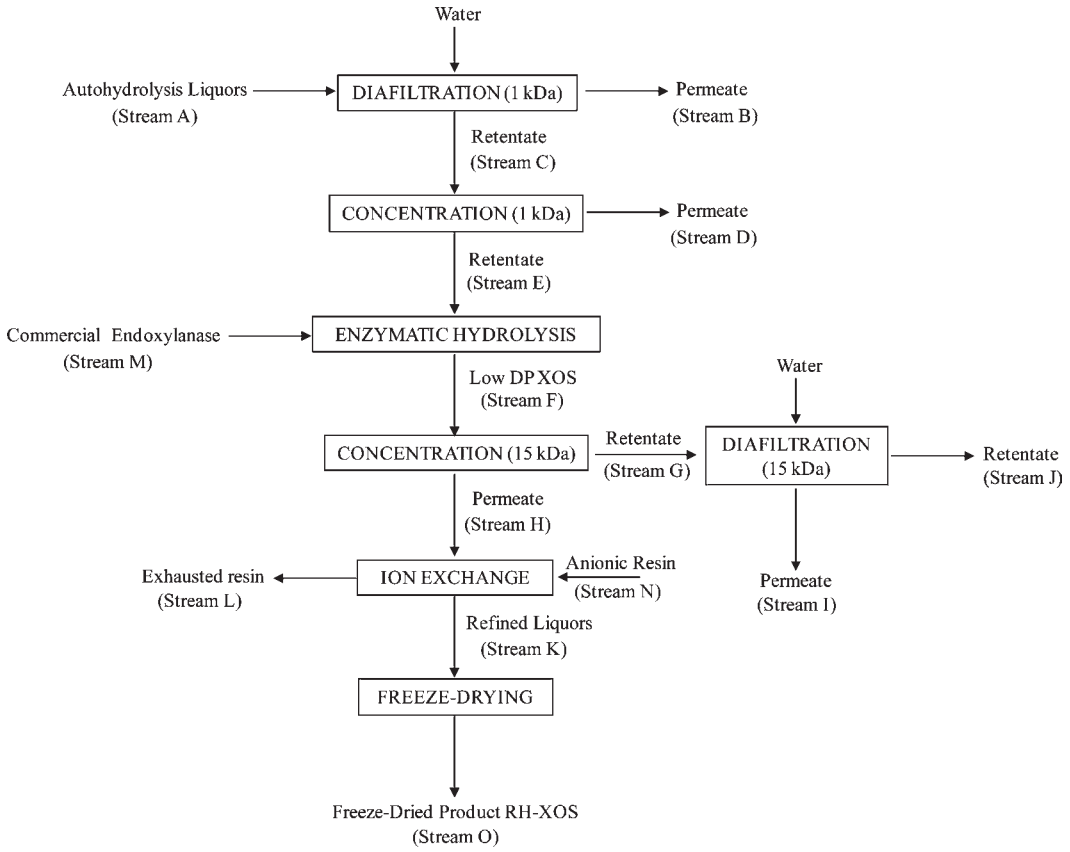

Figure 1. Scheme of the process considered for refining autohydrolysis liquors from rice husks.

products of wide DP range. In order to adapt the average DP of XOS to the preferred values for food applications (*18*), stream E in **Figure 1** was subjected to the action of a commercial endoxylanase under reported operational conditions (*19*), enabling the conversion of high molar mass compounds into shorter oligomers within the preferred range for prebiotic applications (*20*).

Endoxylanase treatments resulted in the generation of oligomers with DP in the range 4−7 as major reaction products, but a small proportion of oligomers with DP > 7 still remained in the medium. The resulting solution (stream F in **Figure 1**) was concentrated using a 15 kDa ceramic membrane, in order to obtain a permeate enriched in low molar mass oligosaccharides and a retentate keeping both high molar mass, slow reacting oligomers and endoxylanases, which could be recycled to the enzymatic hydrolysis stage for recovery. **Table 1** lists compositional data of the ultrafiltered permeate (stream H in **Figure 1**). The percentages of recovery in stream H with respect to stream A were 6.1−18.2% for monosaccharides, 44% for GOS, 42.7% for XOS, 43.3% for Ara, 44.9% for acetyl groups and 34.5% for UA. The mass fraction of ONVC was reduced to 0.11.

As a consequence of the ultrafiltration in mode concentration step, a considerable amount of oligosaccharides remained in stream G (see **Figure 1**). The percentages of recovery in this stream with respect to stream A were 31.5% for GOS, 27.4% for XOS, 36.3% for Ara, 32% for acetyl groups, and 33.5% for UA. As an alternative to improve the recovery of these products, diafiltration with the 15 kDa ceramic membrane was carried out. The resulting permeate (stream I in **Figure 1**) presented the following recovery percents of the target products: 26.6% for GOS, 30.9% for XOS, 23% for Ara, 30.4% for acetyl groups, and 16.4% for UA.

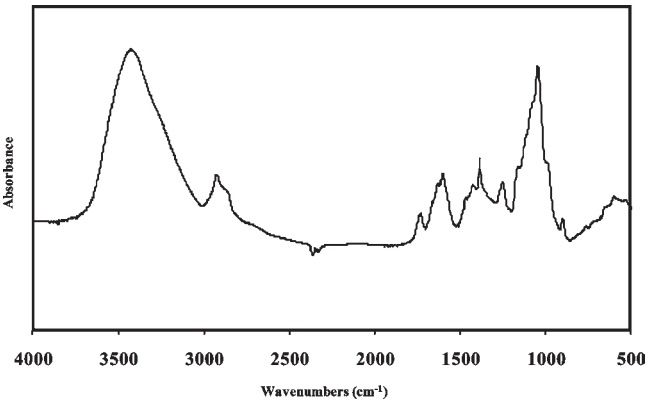

Figure 2. FT-IR spectrum of RH-XOS.

Processing by Ion Exchange. In the final step of the purification scheme, stream H was treated with an anionic exchange resin to yield stream K, which was freeze-dried to give the refined product (stream O, denoted RH-XOS), which was further assessed for *in vitro* fermentability. The percentages of recovery in stream K with respect to stream A were 4.9−14.1% for monosaccharides, 38% for GOS, 37.2% for XOS, 29% for Ara, 31.3% for acetyl groups, 26.7% for UA, and just 2.28% for ONVC. **Table 1** lists the corresponding compositional data. Alternatively, the combined recovery yield of streams K and I with respect to stream A were 6.6−18.2% for monosaccharides, 52.4% for GOS, 52.3% for XOS, 43.6% for Ara, 47.7% for acetyl groups, 38.8% for UA and 2.75% for ONVC.

Structural Characterization of the Purified Product RH-XOS. FT-IR spectroscopy analysis was performed to enable a gross characterization of the carbohydrate and other components

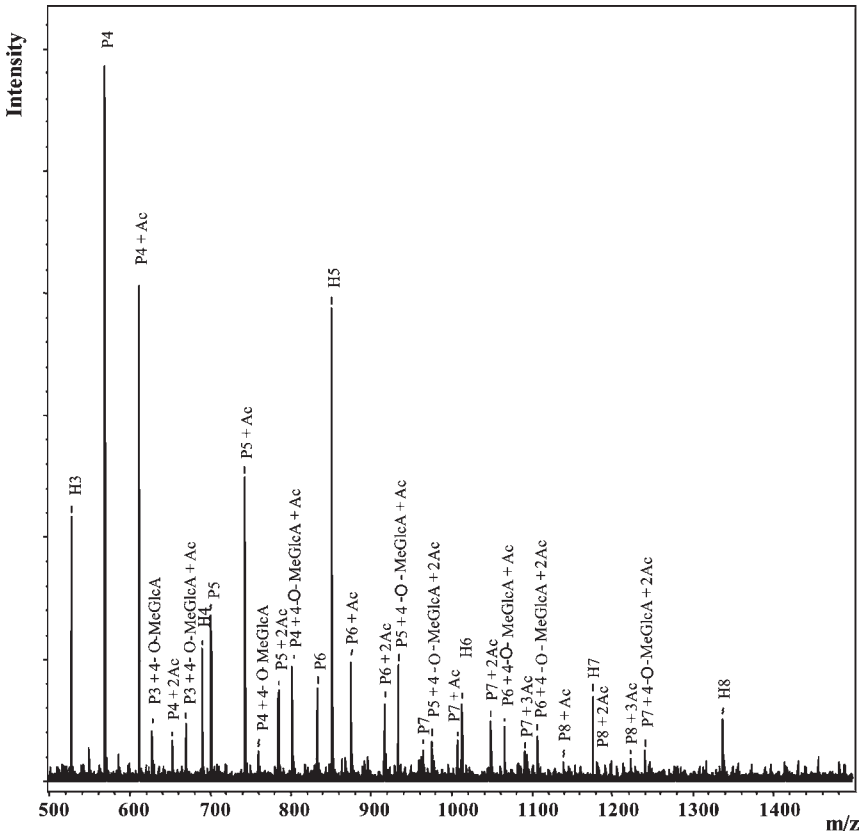

Figure 3. MALDI-TOF mass spectra of RH-XOS.

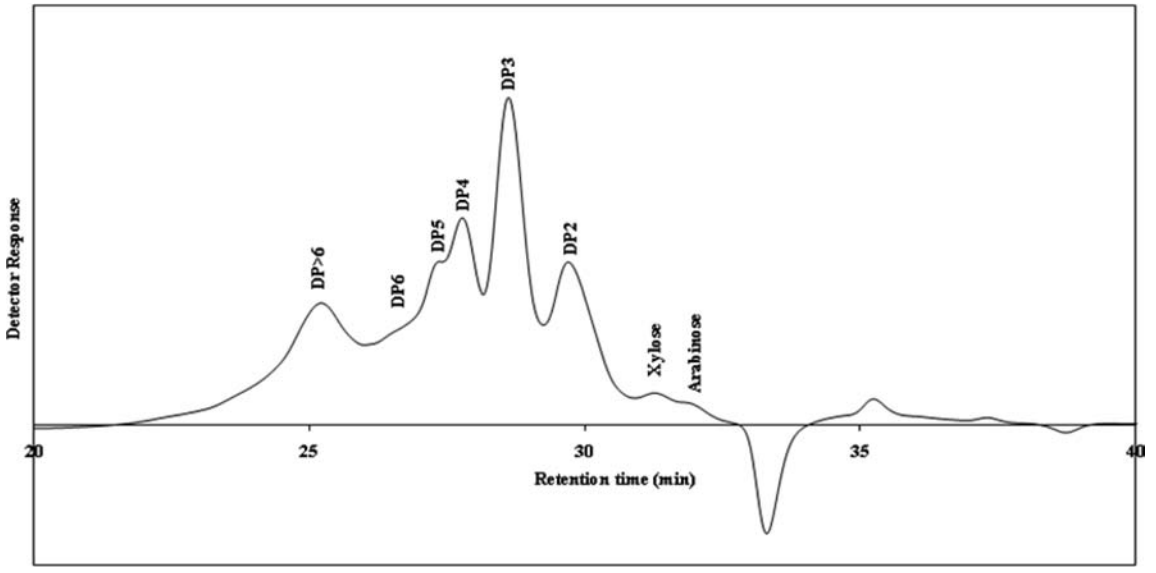

Figure 4. HPSEC elution pattern of RH-XOS.

in relation to the chemical analysis. As seen in **Figure 2**, the pattern of the IR spectrum in the region 1200−1000 cm^{-1} with a maximum band at 1045 cm^{-1} is typical for 4-*O*-methylglucuronoxylan type oligo- and polymers with a very low degree of branching (*21*, *22*). The presence of acetyl groups is indicated by the vibration bands at 1736 cm^{-1} and 1251 cm^{-1} corresponding to the C═O stretching and carbon single bonded oxygen stretching (C−O), respectively. The bands at 1599 cm^{-1} and 1422 cm^{-1} are attributed to asymmetric and symmetric carboxylate stretching bands, respectively, of the uronic acid units. However, the region 1800−1500 cm^{-1} contains also specific absorption bands of proteins and phenolics. The small bands at 1656 and 1536 cm^{-1} are attributed to amide I and amide II vibration bands, respectively, supported by the shoulder at ∼3290 cm^{-1} assigned to ν(N−H) vibration bands, indicated the presence of proteins. The small bands at 1513 cm^{-1} and 1600 cm^{-1} are characteristic frequencies of the skeleton vibration of aromatic ring, and that at 1720 cm^{-1} corresponds to stretching vibration of carboxyl bound to phenolic structures (*23*). Rice husks similarly to other cereal tissues are known to contain heteroxylans with linked phenolic acids (*24*, *25*). The presence of other unsaturated structures resulting from degradation reactions of the

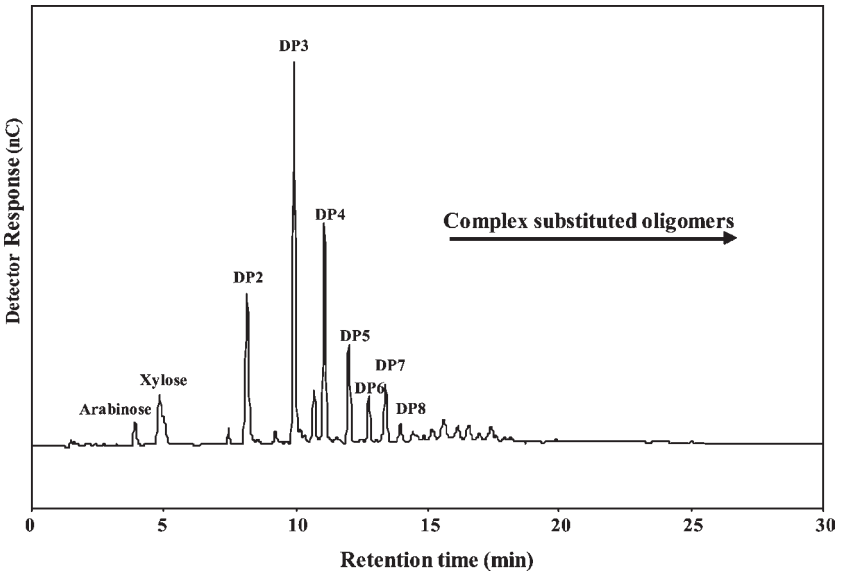

Figure 5. HPAEC-PAD elution profile of RH-XOS.

carbohydrate components during autohydrolysis cannot be ruled out.

The MALDI-TOF mass spectrum of RH-XOS (**Figure 3**) confirmed the presence of a wide range of oligosaccharides containing pentoses, of which the majority is substituted with one or more acetyl groups. According to te compositional data in **Table 1**, most pentoses correspond to xylose. The higher XOS carry up to 3 acetyl groups. It should be stated that oligomers below m/z 500 are not included in the spectrum, due to hindrance of matrix peaks. The acidic oligosaccharides are all representing 4-*O*-methylglucuronic acid (MeGlcA) substituted XOS of which Xyl_{3-4}MeGlcA may carry one acetyl group and the higher oligomers even two acetyl groups. From the sugar composition of RH-XOS, it is anticipated that part of the xylo-oligosaccharides may be substituted with arabinose as well. However, this cannot be substantiated by MS due to equal masses for xylose and arabinose. Furthermore, a homologous series of hexose oligomers (DP 3−8) without acetyl groups can be recognized within the spectrum.

The chemical composition of RH-XOS shown in **Table 1** (stream K/O) indicates that the considered xylooligosaccharide component (after converting XOS, Ara and UA into anhydro units, and acetic acid to acetyl groups) represents nearly 82% of the total carbohydrates present in the final product, whereas the content of GOS (expressed as anhydro units) was about 15%. Posthydrolysis of RH-XOS and further PC analysis of the neutral and acidic sugar analysis (data not shown) confirmed the presence of xylose, arabinose and glucose, revealed, as well as the presence of very small amounts of galactose, and MeGlcA as the only uronic acid component. Considering the UA as MeGlcA, the resulting composition of XOS (in mole ratios) was Xyl:Ara:MeGlcA = 100:4.3:5.4 and the degree of acetylation related to the Xyl*p* units, DS_{Ac}, was 0.14. The estimated molar ratio of XOS and GOS in the RH-XOS product was 87:13.

Because the molar mass distribution and structural features of XOS determine their biological properties (*18*), additional characterization was carried out. HPSEC analysis revealed that the major oligosaccharide contained in RH-XOS presented molar masses in the range 1500 to 200 Da (**Figure 4**). The HPAEC-PAD analysis (**Figure 5**) showed that the oligosaccharides comprised predominately xylooligomers up to DP7. The level of acetylation cannot be revealed, due to online removal of acetyl groups by the high-pH eluent. Uronic acid- and arabinose-substituted XOS are recognized to be present as based on their elution behavior published before (*26*, *27*). Although the response factor of the pulsed amperometric detector will be different for oligomers differing in size and composition, it is clear that a substantial part of RH-XOS consists of dimers and trimers, next to small amounts of monomeric arabinose and xylose. The hexose series of oligomers are not clearly recognized in the HPAEC pattern and most probably are somewhat hidden between the other peaks.

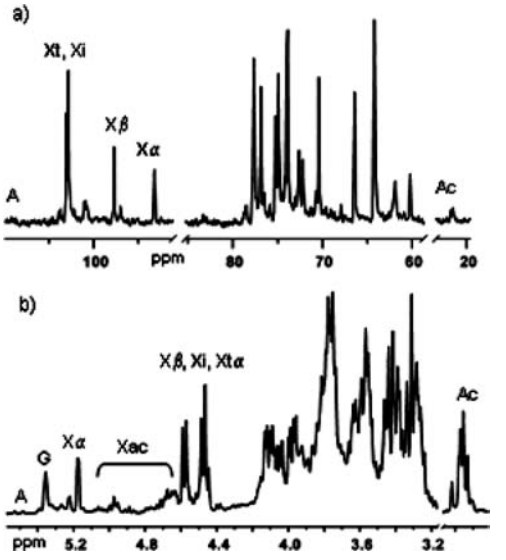

Figure 6. The ^{13}C NMR spectrum (**a**) and ^{1}H NMR spectrum (**b**) of RH-XOS in D_2O measured at 60 °C. The following designations are used: A, terminal α-Ara*f* residue; Xt, Xi, Xβ and Xα, nonreducing end, internal and the reducing end Xyl*p* residues, respectively; Xac, *O*-acetylated Xyl*p* residues; Ac, acetyl groups.

In order to provide a deeper structural assessment, 1D- and 2D-NMR spectroscopy techniques were employed. The signal assignments were based on data published for synthetically prepared xylan-type neutral and acidic oligomers and their acetylated forms (*28*−*30*). The ^{1}H and ^{13}C NMR spectra of RH-XOS illustrated in **Figure 6** resembled those reported for

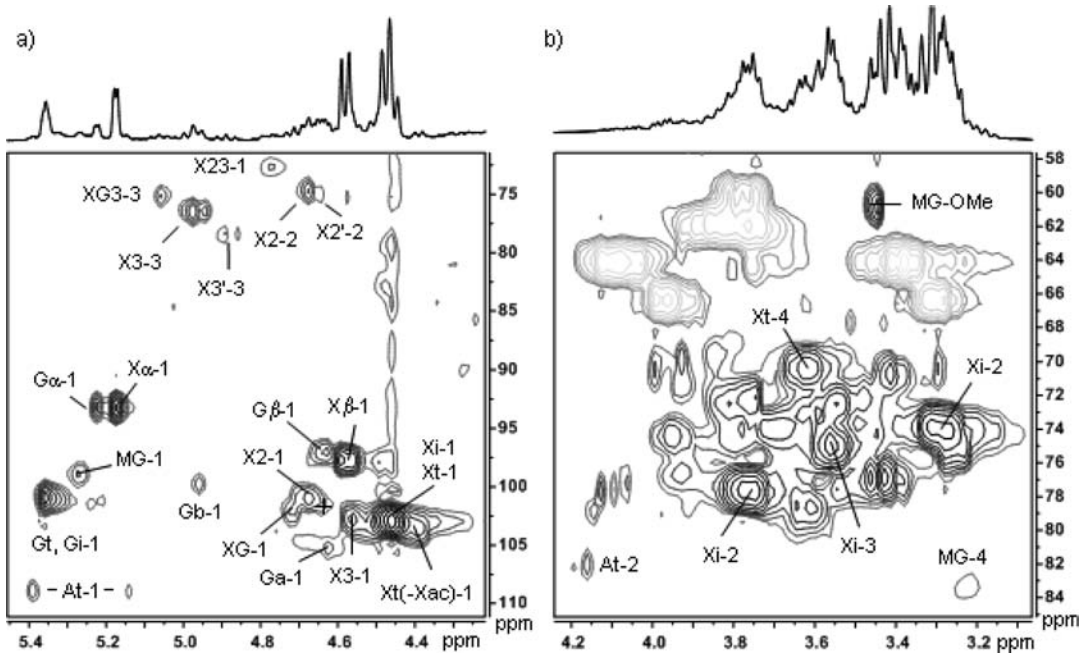

Figure 7. The 2D HSQC spectrum of RH-XOS illustrating (**a**) the anomeric region and (**b**) the other regions. The designations used are summarized in the footnote of **Table 2**. The last number in the cross-peak designation refers to the H and C atoms. The cross (+) indicates the anomeric $^{1}H/^{13}C$ cross peak of X2′ (Xt2).

Table 2. HSQC NMR Cross Peaks of Various Structural Elements of RH-XOS

element[a]	chemical shift, $^{1}H/^{13}C$ (ppm)	assignment	element	chemical shift, $^{1}H/^{13}C$ (ppm)	assignment
Xt(−Xac)	4.40/103.5	H-1/C-1	X23	4.77/73.7	H-2/C-2
Xi, Xt	4.44−4.49/102.8	H-1/C-1	XG	4.71/101.9	H-1/C-1
Xi	3.27/74.1	H-2/C-2	XG3	4.68/102.1	H-1/C-1
	3.75/77.6	H-4/C-4		5.06/75.13	H-3/C-3
Xt	3.43/76.9	H-3/C-3	MG[b]	5.34/98.4	H-1/C-1
Xα	5.17/93.3	H-1/C-1		3.22/83.3	H-4/C-4
Xβ	4.58/97.7	H-1/C-1	Gt, Gi	5.36/100.9	H-1/C-1
X2	4.67/101.0	H-1/C-1	Gα	5.22/93.3	H-1/C-1
	4.67/74.1	H-2/C-2	Gβ	4.63/97.1	H-1/C-1
X2′ (Xt2)	4.63/101.7	H-1/C-1	Gb	5.00/99.8	H-1/C-1
	4.64/75.0	H-2/C-2	At	5.39/108.9	H-1/C-1
X3	4.56/102.5	H-1/C-1		4.16/82.0	H-2/C-2
	4.98/76.5	H-3/C-3	At	5.15/109.0	H-1/C-1
	3.92/76.4	H-4/C-4	Ga	4.62/105.3	H-1/C-1
X3′ (Xt3)	4.89/78.4	H-3/C-3		3.60/79.2	H-4/C-4

[a] Designations used were as follows: MG, 4-*O*-methylglucuronic acid (MeGlcA); Xα and Xβ, Xyl*p* reducing ends; Xi and Xt, Xyl*p* internal and nonreducing ends; Xt(-Xac), nonreducing end Xyl*p* 4-linked to an internal acetylated Xyl*p*; X2 and X2′, 2-*O*-acetylated internal and terminal Xyl*p*; X3 and X3′, 3-*O*-acetylated internal and terminal Xyl*p*; X23, 2,3-di-*O*-acetylated Xyl*p*; XG3, MG 2-*O*-linked and 3-*O*-acetylated Xyl*p*; XG, MG 2-*O*-linked Xyl*p*; Gi and Gt, internal 4-linked and nonreducing end α-Glc*p*; Gα, and Gβ, Glc*p* reducing ends; Gb, 6-linked α-Glc*p* branching unit; At, α-Ara*f* non-reducing end; Ga, β-galactopyranose (Gal*p*). [b] The $^{1}H/^{13}C$ cross peaks for 4-*O*-CH_3 of MeGlcA was at 3.44/60.8 ppm.

partially acetylated 4-*O*-methylglucuronoxylans and those derived from XOS from birchwood (*31*), aspen wood (*32*), *Eucalyptus* wood (*33*) and almond shells (*34*). The molecular and structural heterogeneity of XOS is documented by the large multiplicity of signals in both spectra. As seen in **Figure 6a**, the reducing Xyl*p* end groups (Xα and Xβ) gave relatively strong signals at 97.8−96.9 and 92.8−92.2 ppm, respectively, when compared to those of the internal and nonreducing terminal Xyl*p* (Xi, Xt) in the region 103.8−101.6 ppm, which accorded with the low DP range suggested from the former chromatography analyses. The anomeric region of the ^{1}H NMR spectrum (**Figure 6b**) showed signals of free and acetylated Xyl*p* units. The carboxyl of acetyl groups appeared as 4 signals at 170.3, 170.0, 169.8, and 169.5 ppm, and the methyl of acetyl groups provided also 4 signals at 21.4−22.1 ppm. The corresponding ^{1}H shifts appeared at 2.10−2.22 ppm. The results indicate the presence of different acetylated xylose residues.

The 2D HSQC spectrum (**Figure 7**) was used to identify the various structural elements of RH-XOS. The anomeric $^{1}H/^{13}C$ cross peaks of free and acetylated internal, MeGlcA-substituted (Xi, XG) and terminal (Xt, Xα, Xβ) Xyl*p*, and Glc*p* (G) residues in the region (^{1}H 5.2−4.1/^{13}C 103−92 ppm) and some cross peaks of other protons in the region ^{1}H 3.2−5.0/^{13}C 70−85 ppm are summarized in **Table 2**.

Regardless the low degree of acetylation (DS_{Ac} = 0.14), a distinct cross peak of C-3 of the 3-*O*-acetylated internal Xyl*p* (X3−3) and a very weak one (X3′−3) were observed (**Figure 7a**). The 2-*O*-acetylated Xyl*p* residues gave $^{1}H/^{13}C$ cross peaks assigned to X2−2 and X2′−2 residues as well as the corresponding anomeric ones. The cross peaks of X3′ and X2′ might

correspond to acetylated nonreducing terminal Xyl*p* units in accord with data reported by Kabel et al. (*33*). The cross peaks of the internal and terminal (reducing and nonreducing) Xyl*p* residues are predominating, similarly as those from their other protons (**Figure 7b**). Based on the acetyl group assignments in XOS reported by Teleman et al. (*32*,*35*), the $^{1}H/^{13}C$ cross peaks at 2.22/22.1 and 2.15/21.6 ppm correspond to acetyl groups at position 3 and those at 2.13/21.4 and 2.10/21.4 ppm acetyl groups at position 2. As evidenced with acetylated XOS obtained from hydrothermally treated *Eucalyptus* wood (*33*), migration of the acetyl groups during the isolation process cannot be ruled out. The degree of acetylation and distribution of acetyl groups was estimated by integrating the anomeric cross-peak areas of acetylated (X2, X3, and XG3) and nonacetylated (Xi, Xt, Xα, X*β* and XG) units. The ratio of acetylated to all Xyl*p* units gave a degree of acetylation (DS_{Ac} = 0.12) close to that determined by chemical analysis. Approximately 56% of the acetyl groups are located at position 3, 41% at position 2, and 3% in both positions. The X23 units represent less than 3% of acetylated sugars.

The degree of branching of the XOS by MeGlcA side chains was about three times lower than the acetylation degree. The presence of this structural element, which was predicted by the MALDI-TOF analysis and confirmed by PC analysis, gave a very weak anomeric cross peak (MG). However, the stronger cross peak of the unit Xyl*p* (XG3) indicates a higher proportion of MeGlcA, which was confirmed by the above used calculation yielding the Xyl/MeGlcA ratio 100:5.0 in accord with the chemical analysis.

RH-XOS showed a very low degree of branching by Ara*f* residues, which was documented by two very weak and not well resolved $^{1}H/^{13}C$ cross peaks (At-1 and At-2) attributable to single α-Ara*f* residues attached to the xylan backbone of heteroxylans from cereal bran (*25*).

Based on the HSQC spectrum, the GOS component of RH-XOS was unambiguously assigned to oligomers originating from residual starch. This is documented by the anomeric cross peaks of nonreducing (Gt) and reducing (Gα and G*β*) end and internal (Gi) 4-linked α-Glc*p* residues as well as the branching 6-linked α-GLc*p* unit (Gp) in accord with published data (*36*). The approximate DP of 4 calculated by integration of the cross peaks is in accord with MALDI-TOF analysis. Similarly, GOS were produced during autohydrolysis of various agricultural byproducts (*3*). The very weak anomeric $^{1}H/^{13}C$ cross peaks (Ga) can be attributed to 4-linked *β*-Gal*p* residues from other degraded cell wall polysaccharides (*25*).

Both ^{1}H and ^{13}C NMR spectra (not shown) contained very small signals at 167, 132.4, 130.1, 117, and 114.1 ppm originating from aromatics and other unsaturated structures. Minor signals at δ ~8.4, 7.6−7.5, 7.2, and 6.8−6.7 correspond to such structures (*28*). In accord with the FTIR data, these components are present in XOS in very low amounts.

From the results it can be concluded that RH-XOS contain a very high proportion (~84%) of partially *O*-acetylated XOS with structural features typical of oligosaccharides derived from the methylglucuronoxylan-type hemicelluloses, some carrying single Araf side chains. Similar XOS products, but with a lower content of XOS, were lately isolated by autohydrolysis of rice husks, wheat straw and barley straw, which are all rich in (arabino)glucuronoxylan-type hemicelluloses (*3*).

***In Vitro* Fermentability of Purified XOS and Accumulation of Lactate and SCFA in the Fermentation Media.** In order to assess the prebiotic potential of RH-XOS, fermentation by fecal inocula (FI) was carried out under conditions reported in the literature (*14*). Fermentations were carried out *in vitro*, in order to assess the relative rates at which oligosaccharides are broken down and consumed, and to quantify the production of organic acids in comparative terms.

The time courses of concentrations of oligosaccharides, free monosaccharides, lactate and SCFA (in experiments lasting up to 48 h) were assessed by HPLC. The concentration and pH profiles are shown in **Figure 8**. Consumption of total OS upon fermentation of RH-XOS (see **Figure 9**) resulted in the production of SCFA (acetate, propionate, butyrate, succinate, formiate) and lactate. The increase in cell mass by bacterial growth (data not shown) presented a pattern in close correspondence with substrate consumption.

The decline of OS concentration in the media and the increase in organic acids along fermentations proceeded without accumulation of monosaccharides generated from oligosaccharides, as it has been reported by other authors (*37*). After 12 h, 9.2% of the

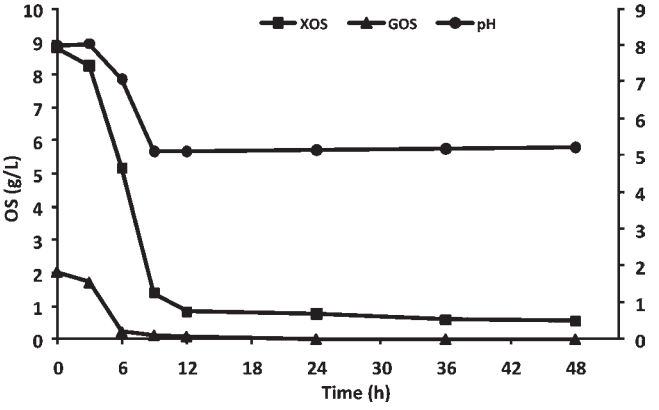

Figure 8. Time courses of oligosaccharide concentrations and pH in fermentation assays.

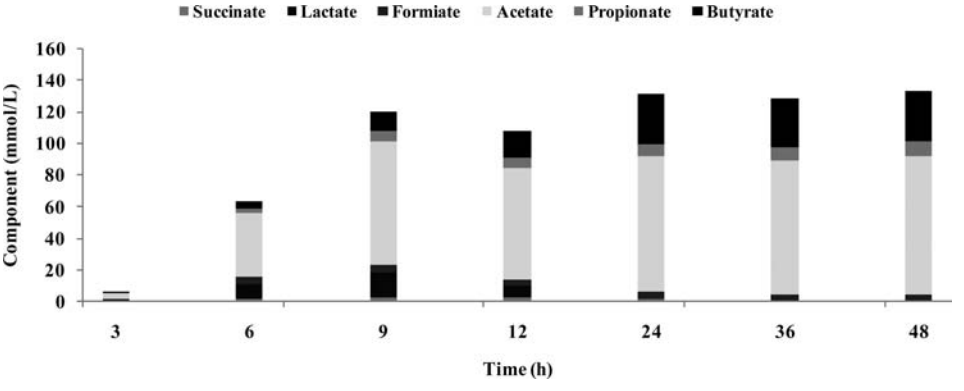

Figure 9. Time courses of the concentrations of SCFA and lactate in fermentation assays.

initial amount of total XOS (calculated as the joint contribution of XOS, Ara and acetyl substituents) remained in the media, in comparison with just 3.8% of unfermented GOS. Longer fermentation times resulted in slow decreases in the concentration of substrates. After 48 h, only 5.8% of the initial XOS and arabinosyl substituents of OS remained in the media, whereas GOS disappeared completely before to 24 h. In comparison with results reported in the literature (*38*), the purified products employed in this work presented faster fermentation kinetics, a fact probably related to their low average DP and limited substitution degree.

The major decrease of pH occurred between 6 and 9 h of fermentation, coinciding with the largest percentage consumption of total XOS (from 43.3 to 83.8%), and with marked increases in the concentrations of SCFA (from 54.5 to 104.1 mmol/L) and lactate (from 9.2 to 15.8 mmol/L). In the case of GOS, the most pronounced concentration decline occurred between 3 and 6 h (consumption from 15.6 to 89% of the initial amount).

Figure 9 presents the time course of SCFA and lactate concentrations. During the first 9 h, the major products were acetate, lactate and butyrate, which were generated in molar ratios of 78.4:15.8:12.9. Additionally, minor amounts of propionate, succinate and formiate were formed. Fermentation times longer than 9 h resulted in increased production of SCFA (from 104.4 up to 133.6 mmol/L), while the lactate decreased from 15.7 mmol/L to total depletion. The sharpest increase in butyrate production occurred between 12 and 24 h, coinciding with the disappearance of lactate and succinate, and could result either from direct assimilation of oligosaccharides or from the consumption of other substrates (for example, lactate) by other microorganisms present in FI (*39*). Acetate and butyrate were the major fermentation end products. The acetogenic potential of the purified products observed in this study is in agreement with other studies (*37*).

In terms of fermentation kinetics, and in agreement with reported results (*38*), two different fermentation stages can be observed: the first one (lasting 9 h) was characterized by a marked drop in pH (from 8 to 5), whereas in the second one (period 9−48 h), the pH remained fairly constant (about 5).

Lactate was typically detected in low concentrations in the first fermentation stage. The increase in lactate production along the first fermentation stage was ascribed to its behavior as an intermediary product of carbohydrate fermentation, which can be converted to acetate, propionate and butyrate by common intestinal bacteria (*40*). Lactate production can be correlated with the participation of lactic acid bacteria (e.g., *Lactobacillus* and *Enterococcus* species) and bifidobacteria early in the fermentation, since they are able to utilize oligosaccharides for producing lactate and acetate, but not butyrate. High generation of acids upon fermentation is considered desirable, because decreased pH limits the growth of potentially pathogenic microorganisms and inhibits the growth of putrefactive bacteria (*41*). Along the second fermentation stage, less carbohydrate degradation was observed, and generation of propionate and butyrate was observed. Even if butyrate can be directly produced from carbohydrates by many different intestinal species, especially clostridia (*38*), the increase in butyrate concentration was observed mainly when all oligosaccharides were already degraded, confirming its production from metabolites.

ABBREVIATIONS USED

Ara, arabinosyl units; FI, fecal inoculum; HPAEC, high-performance anion exchange chromatography; HPSEC, high-performance size exclusion chromatography; MWCO, molecular weight cutoff; NDO, nondigestible oligosaccharides; NVC, non-volatile compounds; GOS, glucooligosaccharides; OS, oligosaccharides; RH-XOS, purified rice husk xylooligosaccharides; SCFA, short-chain fatty acids; UA, uronic acid units; XOS, xylooligosaccharides; XU, xylanase units; FT-IR, Fourier-transform infrared.

LITERATURE CITED

(1) Garrote, G.; Domínguez, H.; Parajó, J. Autohydrolysis of corncob: study of non-isothermal operation for xylo-oligosaccharide production. *J. Food Eng*. **2002**, *52*, 211–218.

(2) Vegas, R; Alonso, J. L.; Domínguez, H.; Parajó, J. C. Processing of rice husk autohydrolysis liquors for obtaining food ingredients. *J. Agric. Food Chem*. **2004**, *52*, 7311–7317.

(3) Nabarlatz, D.; Ebringerová, A.; Montané, D. Autohydrolysis of agricultural by-products for the production of xylo-oligosaccharides. *Carbohydr. Polym*. **2007**, *69*, 20–28.

(4) Kabel, M. A.; Schols, H. A.; Voragen, A. G. J. Complex xylooligosaccharides identified from hydrothermal treated *Eucalyptus* wood and brewerýs spelt grain. *Carbohydr. Polym*. **2002**, *50*, 191–200.

(5) Okazaki, M.; Fujikawa, S; Matsumoto, N. Effect of xylooligosaccharides in the growth of bifidobacteria. *Bifidobact. Microflora* **1990**, *9*, 77–86.

(6) Gibson, G. R.; Probert, H. M.; Van Loo, J.; Rastall, R. A.; Roberfroid, M. B. Dietary modulation of the human colonic microbiota: updating the concept of prebiotics. *Nutr. Res. Rev*. **2004**, *17*, 259–275.

(7) FAO. FAO Technical Meeting on Prebiotics; Rome, Sept 15−16, 2007 (available at: http://www.fao.org/ag/agn/agns/files /Prebiotics_Tech_Meeting_Report.pdf).

(8) Rycroft, C. E.; Jones, M. R.; Gibson, G. R.; Rastall, R. A. A comparative *in vitro* evaluation of the fermentation properties of prebiotic oligosaccharides. *J. Appl. Microbiol*. **2001**, *91*, 878–887.

(9) Taniguchi, H. Carbohydrate research and industry in Japan and the Japanese Society of Applied Glycoscience. *Starch* **2004**, *56*, 1–5.

(10) Vegas, R.; Luque, S.; Alvarez, J. R.; Alonso, J. L.; Domínguez, H.; Parajó, J. C. Membrane-assisted processing of xylooligosaccharide-containing Liquors. *J. Agric. Food Chem*. **2006**, *54*, 5430–5436.

(11) Nabarlatz, D.; Torras, C.; García-Valls, R.; Montané, D. Purification of xylo-oligosaccharides from almond shells by ultrafiltration. *Sep. Purif. Technol*. **2007**, *53*, 238–243.

(12) Gullón, P.; González-Muñoz, M. J.; Domínguez, H; Parajó, J. C. Membrane processing of liquors from *Eucalyptus globulus* autohydrolysis. *J. Food Eng*. **2008**, *87*, 257–265.

(13) Vila, C.; Garrote, G.; Domínguez, H.; Parajó, J. C. Hydrolytic processing of rice husks in aqueous media: a kinetic assessment. *Collect. Czech. Chem. Commun*. **2002**, *67*, 509–429.

(14) Barry, J. L.; Hoebler, C.; Macfarlane, G. T.; Macfarlane, S.; Mathers, J. C.; Reed, K. A.; Mortensen, P. B.; Nordgaard, I.; Rowland, I. R.; Rumney, R. C. Estimation of the fermentability of dietary fibre *in vitro*: an European interlaboratory study. *Br. J. Nutr*. **1995**, *74*, 303–322.

(15) Hartemink, R.; Rombouts, F. M. Comparison of media for the detection of bifidobacteria, lactobacilli and total anaerobes from faecal samples. *J. Microbiol*. **1999**, *36*, 181–192.

(16) Blumenkrantz, N.; Asboe-Hansen, G. New method for quantificative determination of uronic acids. *Anal. Biochem*. **1973**, *54*, 484–489.

(17) Ebringerová, A.; Kramár, A.; Domanský, E. Structural features of (4-O-methylglucurono)xylan from the wood of hornbeam (*Carpinus betulus*, L.). *Holzforschung* **1969**, *23*, 89–92.

(18) Moure, A.; Gullón, P.; Domínuez, H.; Parajó, J. C. Advances in the manufacture, purification and applications of xylo-oligosaccharides as food additives and nutraceuticals. *Process Biochem*. **2006**, *41*, 1913–1923.

(19) Vegas, R.; Alonso, J. L.; Domínguez, H.; Parajó, J. C. Enzymatic processing of rice husk autohydrolysis products for obtaining low molecular weight oligosaccharides. *Food Biotechnol*. **2008**, *22*, 31–46.

(20) Vázquez, M. J.; Alonso, J. L.; Domínguez, H.; Parajó, J. C. Xylooligosaccharides: manufacture and applications. *Trends Food Sci. Technol*. **2000**, *11*, 387–393.

(21) Kačuráková, M.; Belton, P. S.; Wilson, R. H.; Hirsch, J.; Ebringerová, A. Hydration properties of xylan-type structures: an FT-IR study of xylooligosaccharides. *J. Sci. Food Agric*. **1998**, *77*, 38–44.
(22) Kačuráková, M.; Wellner, N.; Ebringerová, A.; Hromádková, Z.; Wilson, R. H.; Belton, P. S. Characterisation of xylan-type polysaccharides and associated cell wall components by FT-IR and FT-Raman spectroscopies. *Food Hydrocolloids* **1999**, *13*, 35–41.
(23) Faix, O. Classification of lignins from different botanical origins by FT-IR spectroscopy. *Holzforschung* **1991**, *45* (Supplement Lignin and Pulping Chemistry), 21−27.
(24) Ishii, T. Structure and functions of feruloylated polysaccharides. *Plant Sci*. **1997**, *127*, 111–127.
(25) Ebringerova, A.; Hromádková, Z.; Heinze, T. Hemicellulose. *Adv. Polym. Sci*. **2005**, *186*, 1–67.
(26) Kormelink, F. J. M.; Gruppen, H.; Viëtor, R. J.; Voragen, A. G. J. Mode of action of the xylan-degrading enzymes from *Aspergillus awamori* on alkali-extractable cereal arabinoxylans. *Carbohydr. Res*. **1993**, *249*, 355–367.
(27) Kabel, M. A.; Schols, H. A.; Voragen, A. G. J. Mass determination of oligosaccharides by matrix-assisted laser desorption/ionization time-of-flight mass spectrometry following HPLC, assisted by on-line desalting and automated sample handling. *Carbohydr. Polym*. **2001**, *44*, 161–165.
(28) Kováč, P.; Alfoldi, J.; Kočiš, P.; Petráková, E.; Hirsch, J. Carbon-^{13}NMR spectra of a series of oligoglycuronic acid derivatives and a structurally related (4-O-methylglucurono) xylan. *Cellul. Chem. Technol*. **1982**, *16*, 261–269.
(29) Petráková, E.; Kováč, P. Synthesis of new methyl O-acetyl-α- and *β*-D-xylopyranosides. *Carbohydr. Res*. **1982**, *101*, 141–147.
(30) Hirsch, J.; Petráková, E.; Hricovíny, M. Stereoselective synthesis and ^{13}C NMR spectra of lower oligosaccharides related to arabinoxylan. *Chem. Pap*. **1989**, *43*, 395–402.
(31) Korte, H. E.; Offermann, W.; Puls, J. Characterization and preparation of substituted xylo-oligosaccharides from steamed birchwood. *Holzforschung* **1991**, *45*, 419–424.
(32) Teleman, A.; Lundqvist, J.; Tjerneld, F.; Stalbrand, H.; Dahlman, O. Characterization of acetylated 4-*O*-methylglucuronoxylan isolated from aspen employing ^{1}H and ^{13}C NMR spectroscopy. *Carbohydr. Res*. **2000**, *329*, 807–815.
(33) Kabel, M. A.; de Waard, P.; Schols, M. A.; Voragen, A. G. J. Location of *O*-acetyl substituents in xylo-oligosaccharides obtained from hydrothermally treated *Eucalyptus* wood. *Carbohydr. Res*. **2003**, *338*, 69–77.
(34) Nabarlatz, D.; Montané, D.; Kardošová, A.; Bekešová, S.; Hríbalová, V.; Ebringerová, A. Almond shell xylo-oligosaccharides exhibiting immunostimulatory activity. *Carbohydr. Res*. **2007**, *342*, 1122–1128.
(35) Teleman, A.; Tenkanen, M.; Jacobs, A.; Dahlman, O. Characterization of *O*-acetyl-(4-*O*-methylglucurono) xylan isolated from birch and beech. *Carbohydr. Res*. **2002**, *337*, 373–377.
(36) McIntyre, D. D.; Vogel, H. J. Two-dimensional Nuclear Magnetic Resonance studies of starch and starch products. *Starch*/*Stärke* **1990**, *42*, 287–293.
(37) Moura, P.; Cabanas, S.; Lourenço, P.; Gírio, F.; Loureiro-Dias, M.; Estevez, M. P. *In vitro* fermentation of selected xylo-oligosaccharides by piglet intestinal microbiota. *LWT-Food Sci. Technol*. **2008**, *41*, 1952–1961.
(38) Kabel, M. A.; Kortenoeven, L.; Schols, H. A.; Voragen, A. G. J. *In vitro* fermentability of differently substituted xylo-oligosaccharides. *J. Agric. Food Chem*. **2002**, *50*, 6205–6210.
(39) Duncan, S. H.; Louis, P.; Flint, H. J. Lactate-utilizing bacteria, isolated from human feces, that produce butyrate as a major fermentation product. *Appl. Environ. Microbiol*. **2004**, *70*, 5810–5817.
(40) Belenguer, A.; Duncan, S. H.; Calder, A. G.; Holtrop, G.; Louis, P.; Lobley, G. E.; Flint, H. J. Two routes of metabolic cross-feeding between *Bifidobacterium adolescentis* and butyrate-producing anaerobes from the human gut. *Appl. Environ. Microbiol*. **2006**, *72*, 3593–3599.
(41) Gibson, G. R.; Roberfroid, M. Dietary modulation of the human colonic microbiota: introducing the concept of prebiotics. *J. Nutr*. **1995**, *125*, 1401–1412.

Received for review December 21, 2009. Revised manuscript received February 5, 2010. Accepted February 11, 2010. The authors are grateful to the Spanish Ministry of Science and Innovation for supporting this study, in the framework of the research Project "Properties of new prebiotic food ingredients derived from hemicelluloses" (reference AGL2008-02072), which was partially funded by the FEDER Program of the European Union. From Slovakia, the Grant SAV-FM-EHP-2008-03-05 and the Slovak Grant Agency (VEGA, Grant No. 2/0062/09) also provided support for this work.